Phycological Research

*Phycological Research* 2009; **57:** 221–237

# Studies on woloszynskioid dinoflagellates V. Ultrastructure of *Biecheleriopsis* gen. nov., with description of *Biecheleriopsis adriatica* sp. nov.

**Øjvind Moestrup,* Karin Lindberg and Niels Daugbjerg**

Phycology Laboratory, Biological Institute, University of Copenhagen, Øster Farimagsgade 2D, DK-1353 Copenhagen K, Denmark

## SUMMARY

An isolate of the very small marine dinoflagellate *Biecheleriopsis adriatica* gen. et sp. nov. (12–15 μm long) has been examined by light, scanning and transmission electron microscopy, combined with partial sequencing of nuclear-encoded large subunit rRNA. *Biecheleriopsis* is a genus of thin-walled dinoflagellates, related to *Biecheleria* and the taxonomic group of *Polarella*, *Protodinium* and *Symbiodinium*, the latter comprising mainly symbionts of marine invertebrates. The mixotrophic *Biecheleriopsis adriatica* is characterized by: (i) a special type of apical furrow apparatus; (ii) an eyespot of Type E *sensu* Moestrup and Daugbjerg; (iii) an unusual type of pyrenoid; and (iv) a spiny resting cyst. Thin sections showed the presence a fibrous connection between the flagellar apparatus and a finger-like extension of the nucleus ('rhizoplast'). It forms a physical connection between the flagella and the nucleus. This unusual structure has previously been considered to characterize the 'true' gymnodinioids, represented by *Gymnodinium* sensu Daugbjerg *et al.* and related forms. However, the apical furrow apparatus and the nuclear envelope of *Biecheleriopsis* are woloszynskioid rather than gymnodinioid. The related genus *Biecheleria* lacks a rhizoplast, and it also lacks a 51-base pair fragment of domain D2 of the large subunit rRNA, which is present in other woloszynskioids. A physical connection between the flagellar apparatus and the nucleus mediated by a fibrous structure is known in other groups of protists, for example, the 'rhizoplast' of many heterokont flagellates, some green algal flagellates, etc. The phylogenetic significance of a rhizoplast in two groups of dinoflagellates that are only distantly related is presently difficult to assess.

Key words: dinoflagellates, phylogeny, phytoplankton, taxonomy, ultrastructure, woloszynskioids.

## INTRODUCTION

In a companion paper we have described the genus *Biecheleria* (Moestrup *et al.* 2009), which comprises a number of thin-walled dinoflagellate species from marine and freshwater ecosystems. While working on that project, we became aware of an isolate from the Adriatic Sea maintained at Institut Francais Recherche Exploration de la Mer (IFREMER), Nantes, France under the name *Gymnodinium corii* J. Schiller, and a closer study of this small species showed it to resemble *Biecheleria*. Here we describe the isolate from light, scanning and transmission electron microscopy, combined with partial sequencing of nuclear-encoded large subunit (LSU) rRNA, and compare the findings with morphological and genetic studies of other woloszynskioids. The isolate superficially resembles *Gymnodinium pygmaeum* Lebour (Lebour 1925) but differs in the position of the nucleus in the cell, in the color of the cell and, perhaps most importantly, in the cingular displacement and the sulcal extension on the epicone. Although superficially similar to *Biecheleria*, the isolate differs ultrastructurally and genetically from this genus, meriting the establishment of a new genus, *Biecheleriopsis* gen. nov.

## MATERIALS AND METHODS

### Origin of material and light microscopy

The isolate was obtained from IFREMER, Nantes, France (as *Gymnodinium corii* J. Schiller). It originates from the Adriatic Sea. Cells are grown in f/2 medium at 32 psu, 20°C and a 12:12 h LD (light : dark) regime or in TL30 medium at 15°C and a 16:8 h LD regime. The culture was subsequently deposited at the Scandinavian Culture Centre for Algae and Protozoa and given the strain number K-0968.

For light microscopy we used a Zeiss (Oberkochen, Germany) Axiophot microscope fitted with Nomarski

**To whom correspondence should be addressed.*
*Email: moestrup@bio.ku.dk*
*Communicating editor: H. Nozaki.*
*Received 8 July 2008; accepted 19 December 2008.*
doi: 10.1111/j.1440-1835.2009.00541.x

interference contrast. Cells were photographed on a Zeiss AxioCam HRc digital camera.

## Scanning electron microscopy

A subsample of the culture was mixed with fixative in a 2:1 volume ratio. The fixative was a 3:1 volume mixture of 2% osmium tetroxide in 30 psu seawater and a saturated aqueous $HgCl_2$ solution. Cells were fixed for 30 min in a small Pyrex glass, and the fixation mixture was then transferred to a Millipore (Billerica, MA, USA) Swinnex holder containing a 5-μm Millipore filter. The cells were rinsed in the holder by the addition of distilled water over a period of 1.5 h, and subsequently dehydrated in the same holder in a graded ethanol series. They were then critical point dried, still within the Swinnex holder, in a Baltec CPD 030 critical point drier. The dry filters were mounted on stubs, coated for 90 s with platinum-palladium and examined in a JEOL (Tokyo, Japan) JSM 6335F field emission scanning electron microscope at the Zoological Museum, University of Copenhagen.

## Transmission electron microscopy

Cells were fixed for embedding and thin-sectioning by mixing equal amounts of culture and a 2% glutaraldehyde in 0.2 M sodium cacodylate buffer containing 0.3 M sucrose, at 15°C. After 80 min in the fridge, cells were concentrated into a clot by centrifugation at 65 *g* for 5 min, and rinsed in three changes of cold buffer (30 min in each change) of decreasing sucrose concentration: 0.3 M sucrose, 0.15 M sucrose, and finally cacodylate buffer only. The material was post-osmicated in cold 2% osmium tetroxide in 0.1 M cacodylate buffer for 2.5 h and subsequently dehydrated in an ethanol series: 30% (20 min), 50% (20 min), 70% (35 min), 96% (20 min), and two changes of absolute ethanol (15 min in each change). The material was brought to room temperature while in 70% ethanol and subsequent steps took place at this temperature. Embedding in Spurr's embedding mixture was preceded by two changes in propylene oxide (5 min in each change) and infiltration overnight in a fume hood in a 1:1 mixture of propylene oxide and embedding medium. This mixture was replaced by two changes of 100% embedding medium (total 3 h), and the material was then flat embedded in resin overnight at 70°C.

Thin sections were prepared on an LKB 8800 ultramicrotome, (LKB, Bromma, Sweden), collected on single-hole slot grids, and stained in uranyl acetate and lead citrate before being viewed and photographed in a JEM-1010 transmission electron microscope at the Biological Institute, University of Copenhagen.

## DNA extraction, polymerase chain reaction and sequence determination of large subunit rRNA

The culture (approximately 10 mL) was grown exponentially prior to being harvested by centrifugation at 1200 *g* for 10 min. Using a Pasteur pipette the resulting pellet was transferred to a 1.5-mL Eppendorf tube and frozen immediately at –18°C. Total genomic DNA was extracted using 2 X hexadecetyltrimethylammonium bromide (CTAB) as described by Daugbjerg *et al.* (1994). Fragments of partial LSU rRNA (approximately 1500 base pairs) were obtained using polymerase chain reaction (PCR) and external primers D1R and ND-1483R (for primer sequences see Scholin *et al.* 1994; Daugbjerg *et al.* 2000). The setup of 50 μL PCR reactions and PCR temperature profile conditions were identical to those outlined in Moestrup *et al.* (2008). We used the Qiagen (Valencia, CA, USA) PCR purification kit to purify the PCR products. The products were sequenced with the Big Dye Terminator Cycle Sequencing kit (ver. 3) and run on an ABI PRISM model 3130 XL automated sequencer at the National History Museum of Denmark, University of Copenhagen. Sequences were assembled and edited by eye using ChromasPro software (ver. 1.41). The nuclear-encoded partial LSU rRNA sequence was submitted to GenBank and given the accession number EU857537.

## Alignment and phylogenetic inference

To infer the phylogeny of the IFREMER isolate we used an alignment already compiled for the study on the recently proposed genus *Biecheleria* (Moestrup *et al.* 2009). Hence, the alignment comprised a diverse assemblage of dinoflagellates with 26 genera and 43 species, including *Biecheleriopsis*. Four ciliates, five apicomplexa and *Perkinsus* formed the outgroup. GenBank accession numbers for in- and outgroup species are given in table 1 of Moestrup *et al.* (2009). The alignment included 1152 base pairs and excluded the highly variable domain D2 (*sensu* Lenaers *et al.* 1989), which presently cannot be aligned unambiguously among the assemblage of dinoflagellates included here. The data matrix was analyzed with Bayesian analysis (BA) using MrBayes ver. 3.12 (Ronquist & Huelsenbeck 2003) and maximum likelihood (ML) using PhyML ver. 3.0 (Guindon & Gascuel 2003). BA was carried out using a general time reversible (GTR) substitution model with base frequencies and substitution rate matrix estimated from the data. Two million Markov Chain Monte Carlo generations with four parallel chains (one cold and three heated) were conducted using the freely available Bioportal (www.bioportal.uio.no). A tree was sampled every 50 generations. Plotting the log likelihood values as a function of generations in a spreadsheet, the lnL

values converged after 20 050 generations. Using 'Are We There Yet' (Wilgenbusch *et al.* 2004) we examined that the BA had been running long enough (plot not shown). The number of generations when the lnL values had converged was used as the burn-in, resulting in 39 600 trees. These were imported into PAUP* ver. 4b10 (Swofford 2003), and a 50% majority rule census tree was constructed. Posterior probability values were also based on this number of trees. We used MrModeltest ver. 2.3 (Nylander 2004) to find the best model of nucleotide substitutions for the LSU rRNA sequences by hierarchical likelihood ration tests. The parameter settings for the gamma shape and the proportion of invariable sites as suggested by MrModeltest were used in PhyML. ML analyses were run at the Montepellier bioinformatics platform. A total of 100 bootstrap replicates were carried out to obtain support values for the tree topology. The consensus program from the Phylip package ver. 3.68 (Felsenstein 2008) was used to obtain a 50% majority rule consensus tree. Posterior probabilities ($PP \leq 1$) and bootstrap values ($\geq$50%) from ML analyses were added to the Bayesian tree shown as Figure 39.

To further examine the phylogeny of dinoflagellates with type E eyespots a second alignment was assembled comprising only these dinoflagellates (see Fig. 39 for included species). Due to their close relationship this alignment also included the highly variable domain D2 and thus, the data matrix was based on 1378 base pairs including introduced gaps. The alignment was analyzed with BA and ML as described above.

## RESULTS

### Biecheleriopsis gen. nov.

*Latin diagnosis*

Dinoflagellata phototrophica parietibus tenuibus et vesiculis amphiesmalibus multis. Vesicula antica elongataque ex latere dorsali ad latus ventrale cellulae extensa. Stigma ad typum E pertinens. Apparatus flagellorum ad extensionem anticam nuclei per structuram fibrillosam affixus. Haec structura ad latus dorsale radicis microtubularis multimembraeque affixa.

Thin-walled phototrophic dinoflagellates whose cells are lined by many amphiesmal vesicles. An elongate anterior vesicle extends from the dorsal to the ventral side of the cell. Eyespot of type E. Flagellar apparatus connected to anterior extension of the nucleus by a fibrillar structure that attaches to the dorsal side of the multi-membered microtubular flagellar root $r_1$.

### Type species: Biecheleriopsis adriatica sp. nov.

*Latin diagnosis*

Cellulae ovatae aut rotundae c. fungiformes. Epiconus hypocono plerumque paulo brevior. Extremitas antica epiconi rotundata interdum parum conica aut pileata. Epiconus dorsali-ventraliter leviter complanatus. Hypoconus asymmetricus et dorsali-ventraliter valde ad antapicem complanatus. Latus sinistrum hypoconi saepe latero dextro brevius. Cingulum *c.* 1.5 plo latitudine sua loco movens. Angulus sinister ventralisque hypoconi manifestus triangularisque processu linguiformi latus dextrum versus et sulcum imbricado. Sulcus ad antapicem attingens profunde excavatus, distantia brevi in epiconum extensus et protuberationem brevem rotundatamque in epicono faciens. Chloroplasti aurei multique, et antici et postici in positione. Pars centralis cellulae nucleo magno occupata. Et hypoconus et hypoconus seriebus latitudinalibus vesicularum amphiesmalium tectus. Cingulum seriebus duobus vesicularum amphiesmalium. Cellulae 13–15 μ longae at 8–13 μm latae.

Cells oval or rounded, more or less mushroom-shaped, the epicone usually slightly smaller than the hypocone, rounded anteriorly, sometimes slightly conical, cap-shaped.

Epicone slightly compressed dorso-ventrally. Hypocone asymmetric, the left side often shorter than the right side and dorso-ventrally compressed towards the antapex. The ends of the cingulum displaced approximately one and a half cingulum widths, the left ventral corner on the hypocone very distinct, triangular, with a tongue-like process directed towards the right and overlapping the sulcus. Sulcus reaches to the antapex, which is deeply excavated. It extends for a short distance onto the epicone, forming a short rounded bulge on the epicone. Many golden chloroplasts, located both anteriorly and posteriorly, the central part of the cell occupied by the large nucleus. Epicone and hypocone both covered by four to five latitudinal rows of amphiesmal vesicles. Cingulum with two horizontal rows of amphiesma vesicles. Cells 13–15 μm long and 8–13 μm wide.

*Light microscopy*

Cell morphology is illustrated in Figures 1 and 2. Cell length 13.1 ± 1.0 μm (range 12.5–15 μm), width 10.3 ± 1.5 μm (range 7.5–12.5 μm) ($n = 6$). Swimming is complex and varied. Generally cells swim rapidly; changing speed and direction abruptly and swimming extremely fast for shorter periods, almost like jumping. Cells display two main types of swimming:

1 Cells rotate around a longitudinal axis, moving in a zig-zag course.
2 Cells swim forward without rotation in a straight or curved line.

After extended examination in the microscope, cells start rotating around a dorso-ventral axis, forming a very characteristic figure like a *Planorbis* snail (Fig. 3).

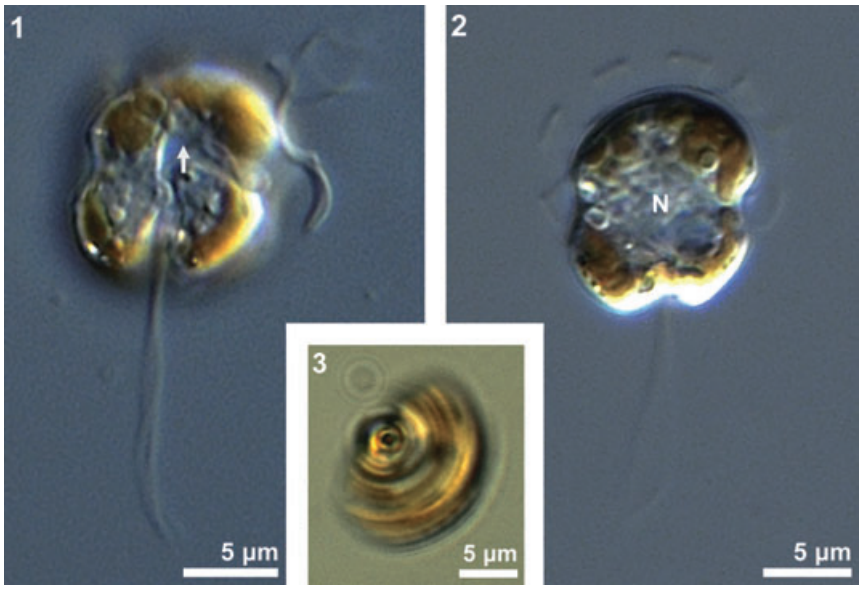


**Figs 1–3.** Light microscopy of *Biecheleriopsis adriatica* gen. et sp. nov. 1. Ventral view of the cell. The sulcus enters the epicone (arrow), and the left ventral corner of the hypocone extends towards the cell's right, covering the flagellar pore area. 2. The cell in Figure 2 has ceased swimming and the detached transverse flagellum is located around the epicone. The central part of the cell is filled with the large nucleus (N) and surrounded by golden chloroplasts. Both figures show the deep antapical excavation. 3. Cell showing *Planorbis*-like movement when rotating around its transverse axis.

When swimming has ceased, flagella are shed and the cingulum disappears.

*Scanning electron microscopy*

Cells are covered by mostly penta- and hexagonal amphiesmal vesicles arranged in latitudinal rows, approximately four to five rows on the epicone and the same number on the hypocone (Figs 4,5,8–10). However, the number of vesicles varies somewhat. Two horizontal rows of vesicles are present in the cingulum. The post-cingular row on the hypocone comprises significantly smaller vesicles (Fig. 7).

In scanning electron microscopy (SEM) the characteristic left ventral part of the hypocone is very distinct. It is shaped almost like a boomerang (Fig. 4), one 'arm' extending over the flagellar pore area, almost reaching the ventral ridge area. A lateral view of the hypocone (Fig. 8) illustrates the size and shape difference between the right and left side, the latter being shorter and strongly dorso-ventrally compressed.

The deeply invaginated sulcus terminates on the epicone in a single large rounded vesicle (two asterisks in Figs 4,6). The antapical excavation extends onto the dorsal side of the hypocone (Figs 5,9). The transverse flagellum often appears to be too large to fit into the cingulum and is usually seen protruding (Figs 5,8,9). This is also visible in light microscopy (LM) (not illustrated) where the flagellum appears as a broad wavy band circumscribing the cell.

The apical furrow apparatus is rather short, and comprises a narrow elongate apical vesicle (EAV), approximately 3 µm long, which extends from the mid ventral side of the epicone over the apex to the left dorsal side (Figs 4,9–12). The EAV is ornamented with a central row of approximately 18 small knobs. On each side it is bordered by one (or two, not shown) elongate but somewhat broader vesicles (Fig. 12). A very small vesicle is located at the ventral end of the EAV (Fig. 10, arrowhead in Fig. 12).

The cell illustrated in Figure 13 is almost certainly a resting cyst, but only a few were seen.

## Transmission electron microscopy

Figures 14 and 15 are low-power micrographs to show cells in longitudinal (Fig. 14) and transverse sections (Fig. 15). All major organelles are visible in the dorsoventrally slightly flattened cell, including the central/dorsal nucleus, which may be seen even at this low magnification to extend towards the basal bodies of the flagella (bb). The chloroplasts are located along the cell periphery, and the eyespot just posterior to the flagellar insertion (Fig. 14). The sectioned cell in Figure 14 also illustrates a food vacuole with unidentifiable contents. In addition the cell contains lipid droplets, seen as opaque bodies of different sizes (Figs 14,15). The chloroplast contains several pyrenoids. As many as three have been seen in a single section, indicating that several are present. They belong to the projecting type (Figs 16–18), surrounded on the outside by a semicircular starch grain (seen best in Fig. 18). At the base of the pyrenoid are rounded vesicles, which Figure 19 shows to be formed by the swollen ends of thylakoids. At least one of the vesicles extends into the pyrenoid matrix as a U-shaped structure (Fig. 17, less clearly visible in Fig. 18, right).

The amphiesma was difficult to study as the amphiesma vesicles had mostly broken during fixation. The connections between the outer and the inner amphiesma membrane had disappeared, but the

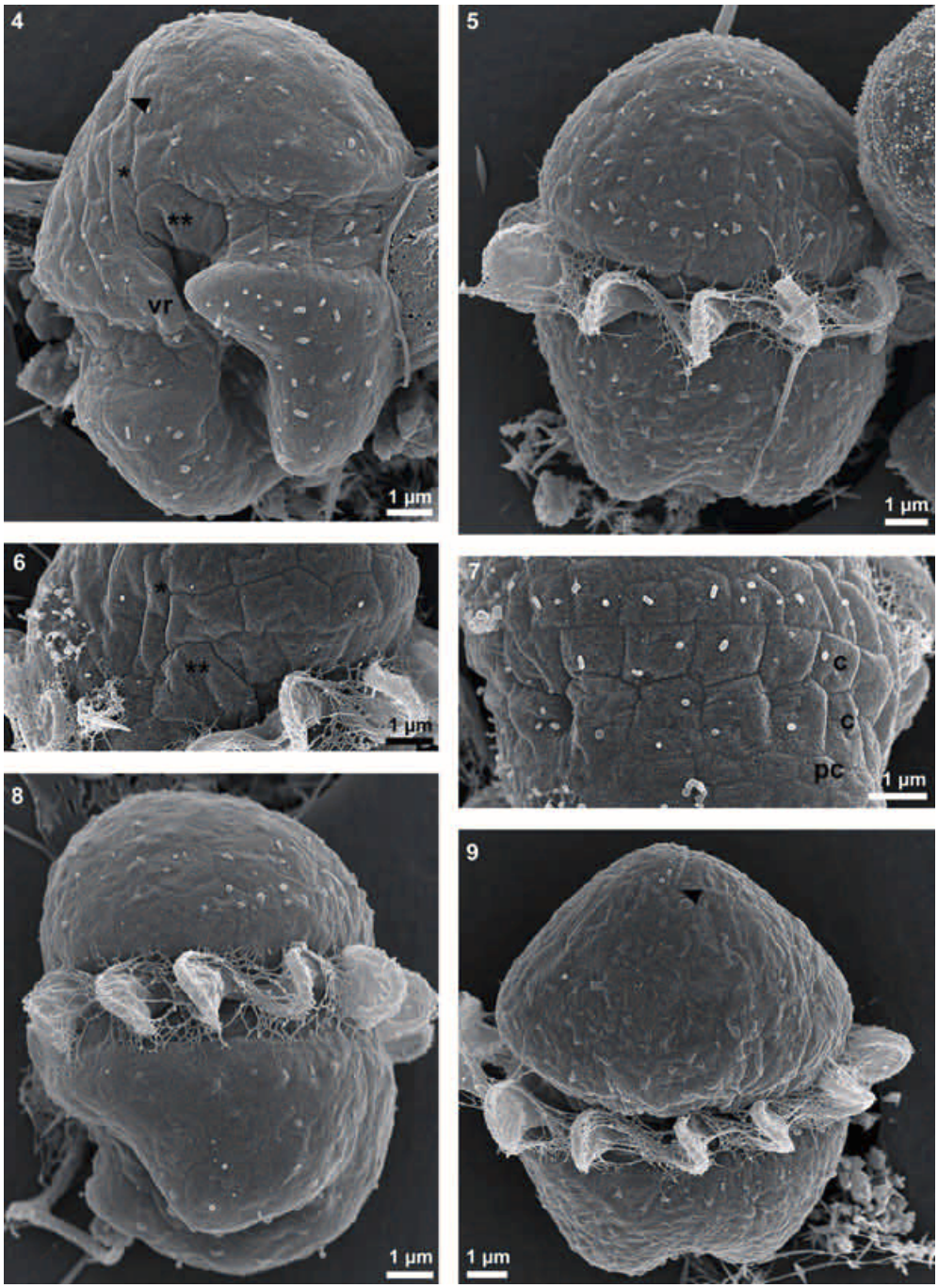


**Figs 4–9.** Scanning electron microscopy of *Biecheleriopsis adriatica* gen. et sp. nov. 4. Slightly oblique ventral view showing the general asymmetry of the cell and the ventral termination of the elongate apical vesicle (EAV). The deep antapical excavation is seen in dorsal view in Figures 5 and 9. The sulcus remains deeply invaginated until reaching the epicone where it terminates in a single large amphiesmal vesicle (two asterisks, Fig. 4), also visible in another cell in Figure 6. Figure 5 is a dorsal view of a cell with a rounded epicone showing the conspicuous transverse flagellum (see also Figs 8,9). 7. The two horizontal rows of cingular vesicles; the upper vesicles are pentagonal and the lower are hexagonal. The vesicles in the postcingular row are significantly smaller than other amphiesmal vesicles. 8. Left lateral view showing the shorter and more dorso-ventrally compressed left side of the hypocone. 9. Upper dorsal view of cell with cone-shaped epicone showing the dorsal extension of the EAV. Arrowheads mark the EAV. c, cingular plates; pc, postcingular plates; vr, ventral ridge area. The large vesicle at the upper end of the sulcus has been marked by two asterisks, while the single asterisk marks the adjacent elongate vesicle that almost reaches the EAV (see also Figs 10–13).

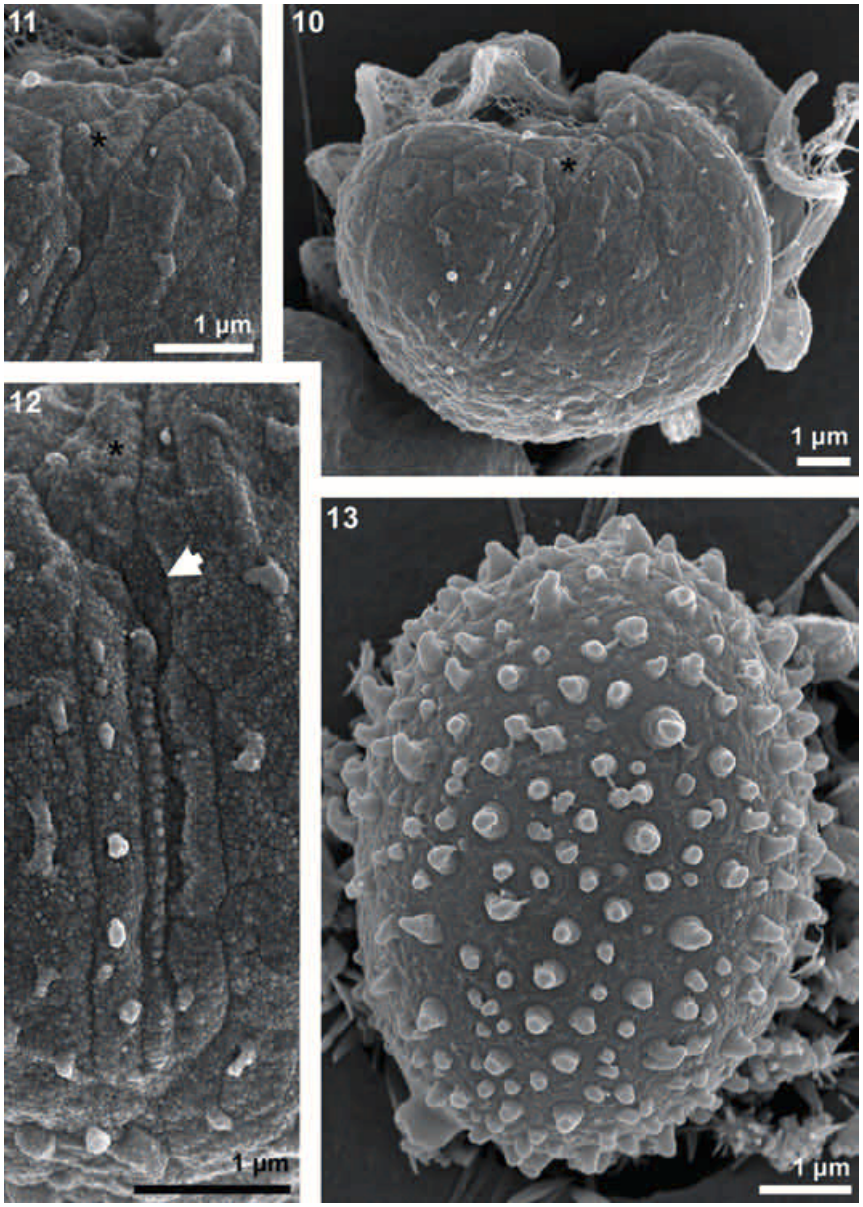


**Figs 10–13.** Scanning electron microscopy of *Biecheleriopsis adriatica* gen. et sp. nov. 10–12. The elongate apical vesicle (EAV). 10. Apical view showing the orientation of the EAV. 11. Higher magnification to show the ventral termination and adjacent vesicles. 12. High magnification showing the construction of the EAV with the central, narrow, elongate vesicle ornamented with small knobs, bordered on each side by an elongate vesicle. The small vesicle at the ventral end has been marked by an arrowhead. 13. Probable resting cyst.

breakage points were still visible. Each amphiesma vesicle contained a single, thin component, which in thickness approximates the amphiesmal membranes, that is, <5 nm. A careful search was made to identify the apical furrow apparatus, for comparison with other woloszynskioids (Figs 20,21). As shown in SEM, the apical furrow apparatus comprises a single EAV, 0.2 µm wide in Figure 20, lined on each side by a slightly wider neighboring vesicle (nv) (both approximately 0.4 µm wide in the figure). The EAV is subtended by a set of 4 + 1 microtubules (large arrow, Fig. 20).

The single microtubule is located near the edge of an opaque plate, which measures approximately 0.10 × 0.01 µm. Above the group of four is another, thinner opaque plate, and a sheet of similar opaque material is present beneath the adjacent part of the neighboring vesicles (Figs 20,21).

The eyespot is rather large and conspicuous, comprising approximately six cisternae with brick-like material (Fig. 14, in more detail in Fig. 22). Superficially it resembles a large Golgi body during formation of organic scales as in many scale-bearing flagellates.

Each cell contains two pusule systems (Figs 23,25,27), each pusule divided into two parts. The inner part is represented by a series of tubules (p in Figs 23,25), the tubular membrane closely lined by a vacuole (v in Fig. 24). The tubules join to a common pusule canal (cpc in Fig. 26 and lowermost part of Fig. 25), which in turn leads to one of the flagellar canals, one pusule canal into each of the transverse (tfc) and longitudinal flagellar canals (lfc), respectively. Figure 26 shows seven tubules at their point of fusion with the pusular canal. While the canals did not contain any noticeable material, the tubules usually contained

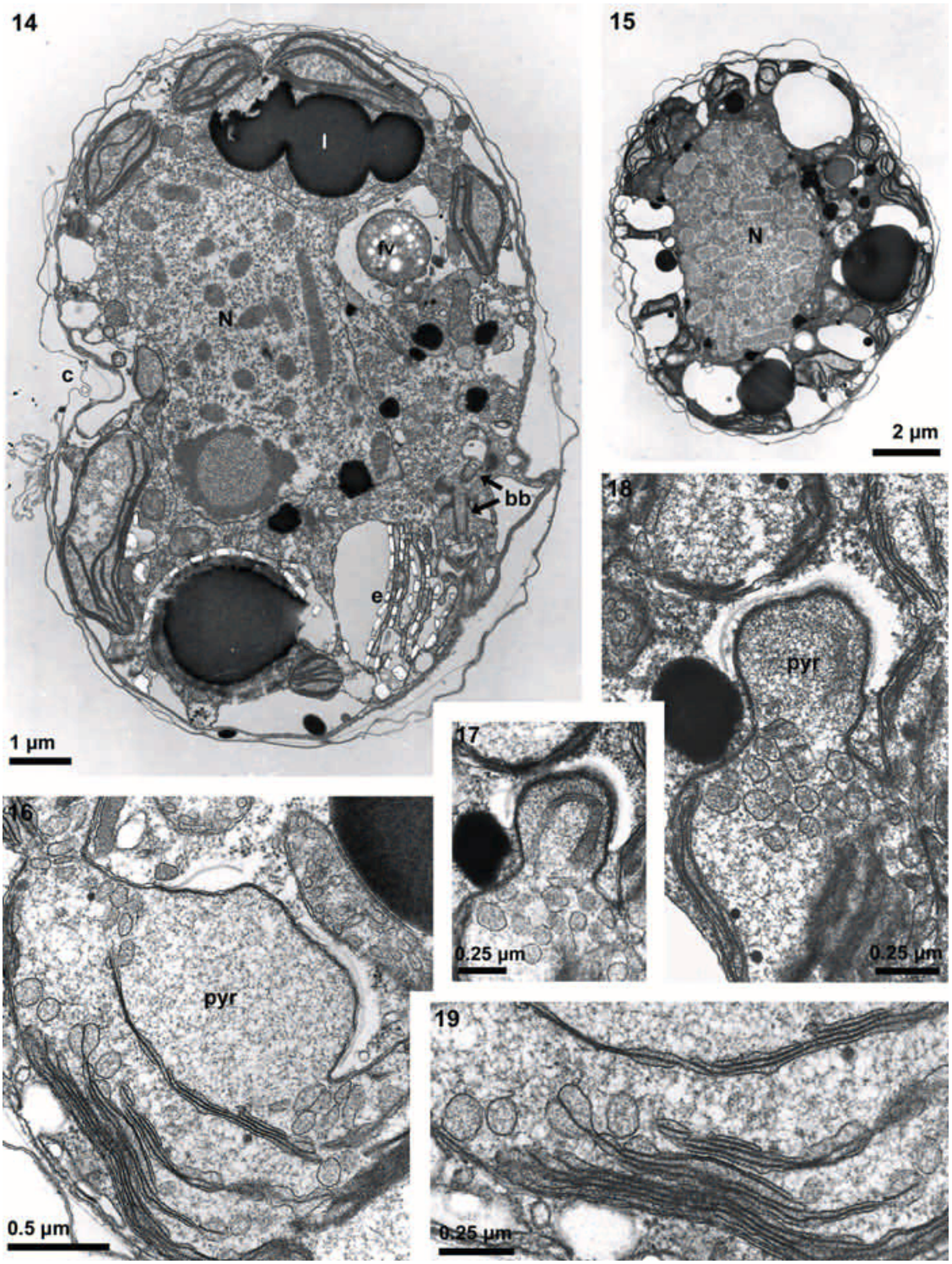


**Figs 14–19.** General overview and pyrenoid of *Biecheleriopsis adriatica* gen. et sp. nov. 14. Cell in longitudinal section. 15. Epicone in transverse section. Most organelles are visible in the cell which is distinctly flattened dorso-ventrally. The nucleus is centrally located, mostly in the epicone. Many chloroplast profiles are present along the cell periphery. 16–19. Details of the pyrenoid, which has an unusual structure. The terminal ends of the thylakoids in the region beneath the pyrenoid matrix are swollen, and a few swellings penetrate into the pyrenoid matrix. A single swelling is visible in longitudinal view in Figures 17 and 18, which are from the same cell. The pyrenoid is capped on the outside by a thin opaque layer, probably starch. bb, flagellar basal bodies; c, cingulum; e, eyespot; fv, food vacuole; l, lipid globule; N, nucleus; pyr, pyrenoid.

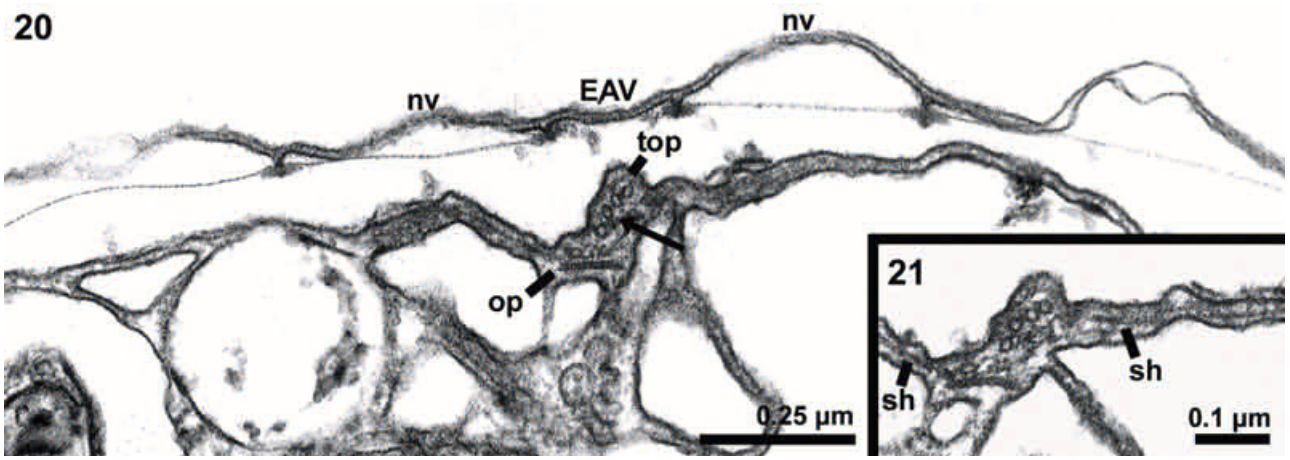


**Figs 20,21.** The anterior end of *Biecheleriopsis adriatica* gen. et sp. nov. The apical elongate vesicle (EAV) is lined on each side by a narrow vesicle (nv, neighbouring vesicle). Below the EAV is a system of 4 + 1 microtubules (arrow), associated with opaque bars (plates). The cytoplasmic side of the neighboring amphiesma vesicles are lined, at least for part of their width, by a very thin, opaque sheath-like structure. The amphiesma vesicles broke during the fixation procedure but the junctions between the vesicles are still visible. Each vesicle contains a very thin opaque plate. op, opaque plate; sh, sheet; top, thinner opaque plate.

a very fine-grained substance, mostly located along the limiting membrane. The nuclear envelope is penetrated with numerous nuclear pores (Fig. 29).

The two flagella insert at an angle of approximately 140 degrees to each other (Fig. 30). Four flagellar roots have been identified. Root $1 = r_1$ (terminology *sensu* Moestrup 2000) is multi-stranded and extends from the basal body of the longitudinal flagellum (flagellum 1) (Figs 28,34,35), passing in the antapical direction along the sulcus in the space between the eyespot and the cell periphery. As in several related species, the microtubules of $r_1$ are overlain in this narrow space by a system of thin parallel fibers, which may be distinguished in Figure 23, arrowhead bottom left. The system of fibers traverses the sheet of microtubules at an angle of approximately 50 degrees. The $r_1$ root is a central structure in the cell, and associates with many other structures. Proximally it joins to root $r_4$ by the very distinct banded src (striated root connective) seen best in Figures 34 and 35 and in more oblique sections in Figures 23 and 25. The src attaches on one end to the striated component of root $r_4$, and on the other end to the microtubules of root $r_1$ closest to the basal body (Figs 34,35). The src comprises several bands of different thickness. The most prominent band is located centrally and comprises two plates. A slightly more prominent band also comprising two plates is situated midway between the central band and root $r_4$. In the corner between the src and $r_1$ is an opaque structure, which extends dorsally into the cell to establish contact with a finger-like projection from the nucleus (npr in Fig. 28). This nuclear connector (nc) is undoubtedly the single-most unexpected structure observed in *B. adriatica* and is illustrated in some detail. As shown in Figures 32 and 33 the fibers of the nuclear connector emanate from at least 10 and probably more microtubules of root $r_1$. At the other end, the fibers ensheath the nuclear projection. We have occasionally seen indications of a cross-banding of the nuclear connector (arrowheads in Fig. 31).

Figure 34 also shows the $r_2$ root, which from the basal body of the longitudinal flagellum extends towards but bypasses the collar of the longitudinal flagellum canal (clf, seen as an opaque band in Fig. 34). Root $r_3$ extends from the basal body of the transverse flagellum; the sheet of microtubules nucleated by the single microtubule of this root is very conspicuous along the canal of the transverse flagellum (Figs 28,34, in Fig. 23 seen as a curved band near the canal of the transverse flagellum). Root $r_4$ is also conspicuous, comprising a single microtubule and a cross-banded component that extends from the basal body of the transverse flagellum to the cytoskeleton beneath the cell periphery (Fig. 36), a distance of approximately 1.75 µm.

The basal bodies are interconnected by a cross-banded fiber that extends from the proximal end of basal body 1 near the innermost microtubules of $r_1$, to establish contact with the side of basal body 2 (Fig. 34 and in more detail in Fig. 35). Another structure observed in the flagellar apparatus area is a curved double-banded structure located outside two of the triplets in basal body 2 (arrow Fig. 28). This double band, which is very conspicuous, has apparently not been reported in other dinoflagellates; it curves over an opaque body next to one of the triplets.

The culture of *Biecheleriopsis* grew rapidly and flagellar replication was observed in several cells. Figures 37 and 38 are from a series of sections through a replicated set of basal bodies. Two new basal bodies (nbb) are formed *de novo* near and parallel to the

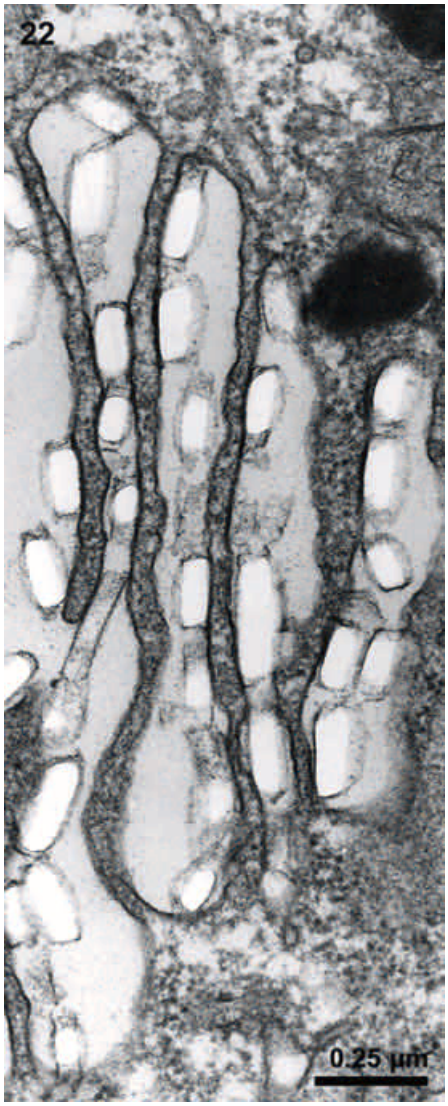


**Fig. 22.** The eyespot of *Biecheleriopsis adriatica* gen. et sp. nov. The stigma is a Golgi body-like structure in which each cisterna is filled with brick-like material, seen here as translucent boxes.

original basal body of the transverse flagellum (obb2). Both new basal bodies are lined by short, single microtubules, associated with basal body triplets (arrows in Figs 37,38). The involved triplets are separated on one side by three and on the other by four triplets, corresponding to attachment points of roots $r_3$ and $r_4$ of the mature, transverse flagellum basal body. It is more difficult to explain the presence and function of a sheet of approximately six microtubules in the area between basal body 2 and one of the newly formed basal bodies (Fig. 37 arrowhead, Fig. 38). Other, opaque bands visible near the newly-formed basal body indicate that this small rapidly-dividing species may be suitable for more detailed studies of flagellar formation and replication in dinoflagellates, to extend the results by Heimann *et al.* (1995).

## Phylogeny

The LSU rRNA data matrix provided no support from posterior probabilities (PP) or bootstrap values for the relationship of the deepest diverging lineages (Fig. 39). However, the species of particular interest to this study received the highest branch support possible (i.e. PP = 1 in BA and bootstrap = 100% in ML). Hence, the phylogenetic inference strongly favored monophyly of dinoflagellates possessing type E eyespots *sensu* Moestrup and Daugbjerg (2007). Within the dinoflagellates having this type of eyespot the bipolar *Polarella glacialis* took a basal position as it formed a sister taxon to two clades; one comprised *Protodinium simplex* (CCMP 418) and *Symbiodinium* spp. (i.e. the recently proposed *S. natans* and an unidentified Australian species belonging to *Symbiodinium* lineage C). The other clade comprised *Bicheleria* (namely, *B. baltica* and *B. pseudoplaustris*) and *Biecheleriopsis adriatica* (Fig. 39). The branching pattern for dinoflagellates with type E eyespots was moderate to well supported in BA (PP: 0.62–0.96) but with low or missing support in ML bootstrapping (<50% or 75–78%). The very short branch lengths in this part of the tree also indicated this. To further elucidate the relationship between *Biecheleriopsis adriatica* and the other dinoflagellates with type E eyespots a second LSU rRNA alignment was constructed that included the highly variable domain D2. Based on the tree topology illustrated in Figure 39, *Baldinia anauniensis* (with type B eyespots) formed a sister to dinoflagellates with type E eyespots. Hence *B. anauniensis* was used as the root in phylogenetic analyses based on the second alignment. The tree obtained using BA is shown as Figure 40. Again *Polarella* formed a basal clade but *Biecheleriopsis adriatica* in this analysis formed a sister taxon to *Biecheleria* spp., *Protodinium* and *Symbiodinium* spp. Posterior probabilities supporting the tree topology were fairly high (PP: 0.81–1.0) whereas ML bootstrap values were ≤53% except for the relationship between the two species of *Biecheleria,* which was supported by 94% (Fig. 40). Despite the inclusion of domain D2 a more robust branching pattern was not achieved for dinoflagellates with type E eyespots at least in ML bootstrap analyses. Yet the phylogenetic analyses based on the second alignment did not approve of a sister group relationship between *Biecheleria* spp. and *Biecheleriopsis adriatica* when including an additional 226 base pairs.

# DISCUSSION

## Identity of the isolate from IFREMER

The description by Lebour (1925) of her new species *Gymnodinium pygmaeum* is brief and accompanied by a

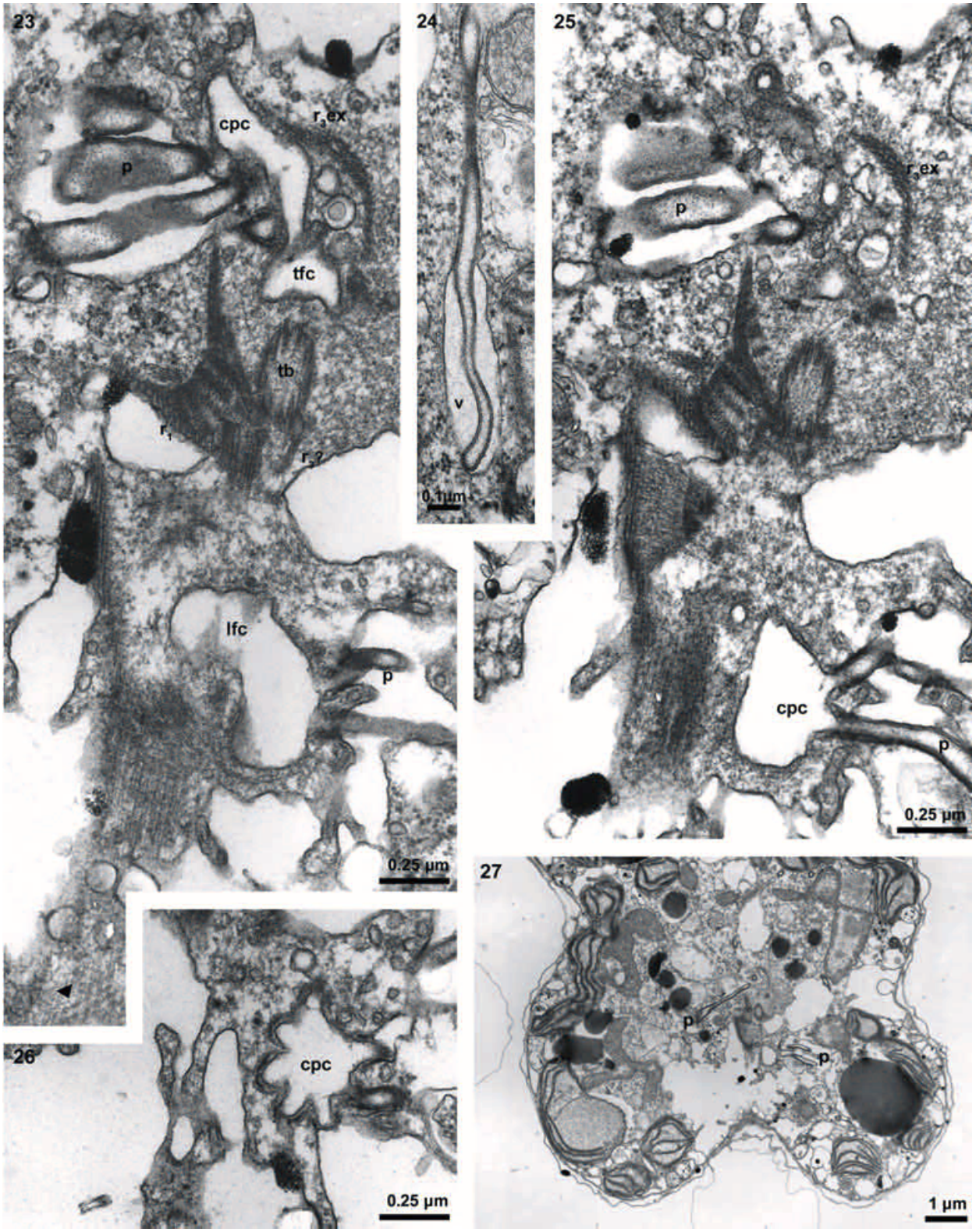


**Figs 23–27.** The pusule apparatus of *Biecheleriopsis adriatica* gen. et sp. nov. Each cell contains two pusules (p), connected to the exterior via common pusule canals (cpv), seen at low magnification in Figure 27. One pusule canal connects to the canal of the transverse flagellum (tfc, Fig. 23), the other to the canal of the longitudinal flagellum (lfc, Fig. 23). At least seven tubes empty into each common pusule canal (cpc, Fig. 26), each tube lined by closely appressed vacuoles (v), seen at high magnification in Figure 24. The arrowhead in Figure 23 indicates the system of fine fibers that accompanies flagellar root $r_1$, oriented at an angle of approximately 50°. $r_3$ex = extension of root $r_3$ in Figures 23 and 25.

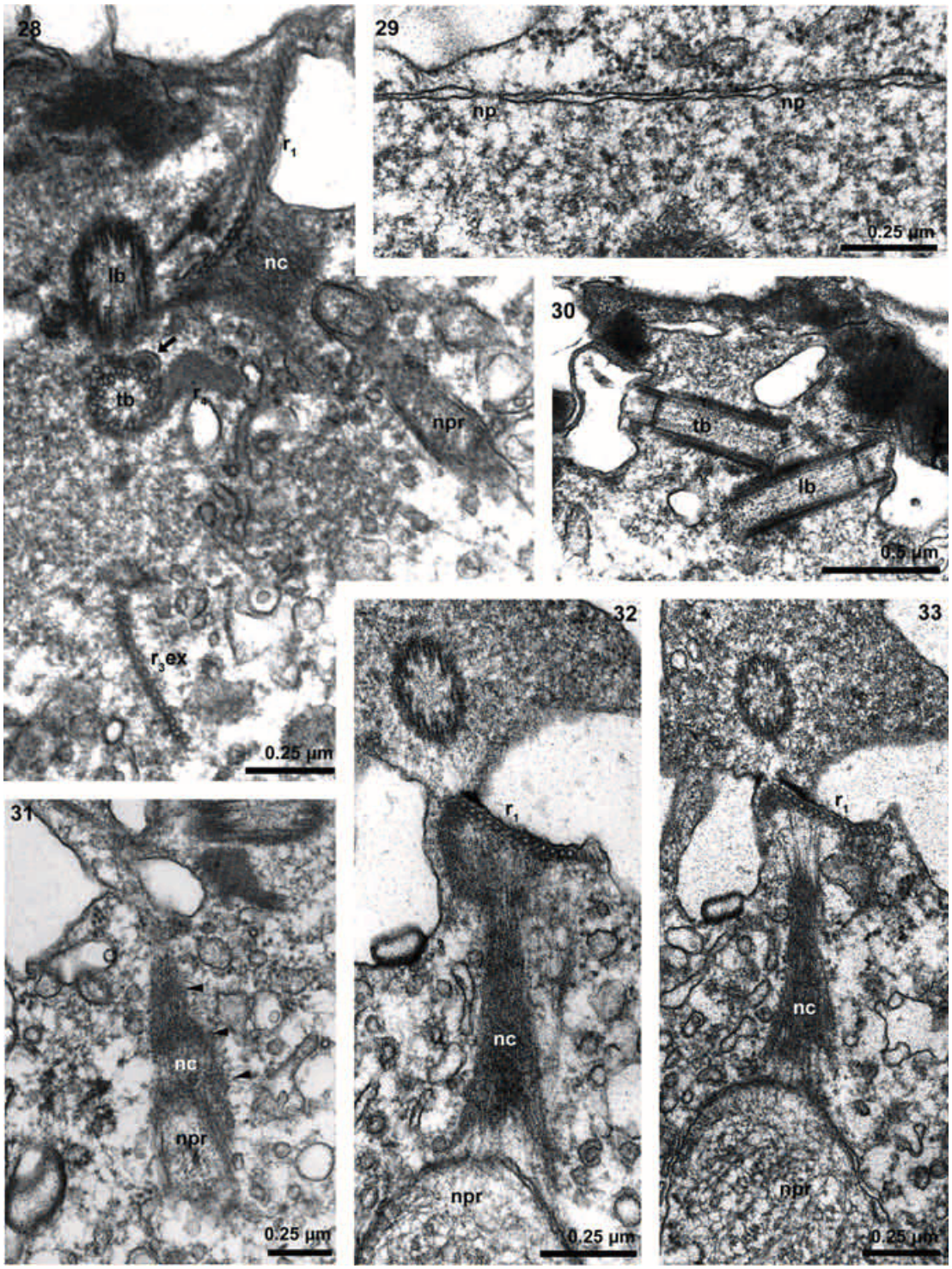


**Figs 28–33.** Details of the nucleus and the nuclear connector of *Biecheleriopsis adriatica* gen. et sp. nov. 28. Overview showing the two flagellar basal bodies (lb, tb), two of the microtubular flagellar roots ($r_1$ and $r_4$) and part of the extension of $r_3$ ($r_3$ex). A conspicuous opaque structure emanates from the dorsal side of $r_1$ towards a finger-like projection of the nucleus (npr). The arrow indicates a compound structure of two concentric half circles surrounding opaque material associated with a basal body triplet. This structure has apparently not been seen previously in dinoflagellates. 29. The nuclear envelope with typical nuclear pores in the envelope (np). 30. The two basal bodies insert at an acute angle to each other, the basal body of the transverse flagellum (tb, flagellum 2) terminating on the outside of the basal body of the long flagellum (lb, flagellum 1), midway along the length of lb. 31–33. Details of the fibrous nuclear connector (nc), which extends from several microtubules of flagellar root $r_1$ to ensheath a more or less finger-like projection of the nucleus (npr). The connector sometimes gives the impression of being transversely striated (arrowheads in Fig. 31).

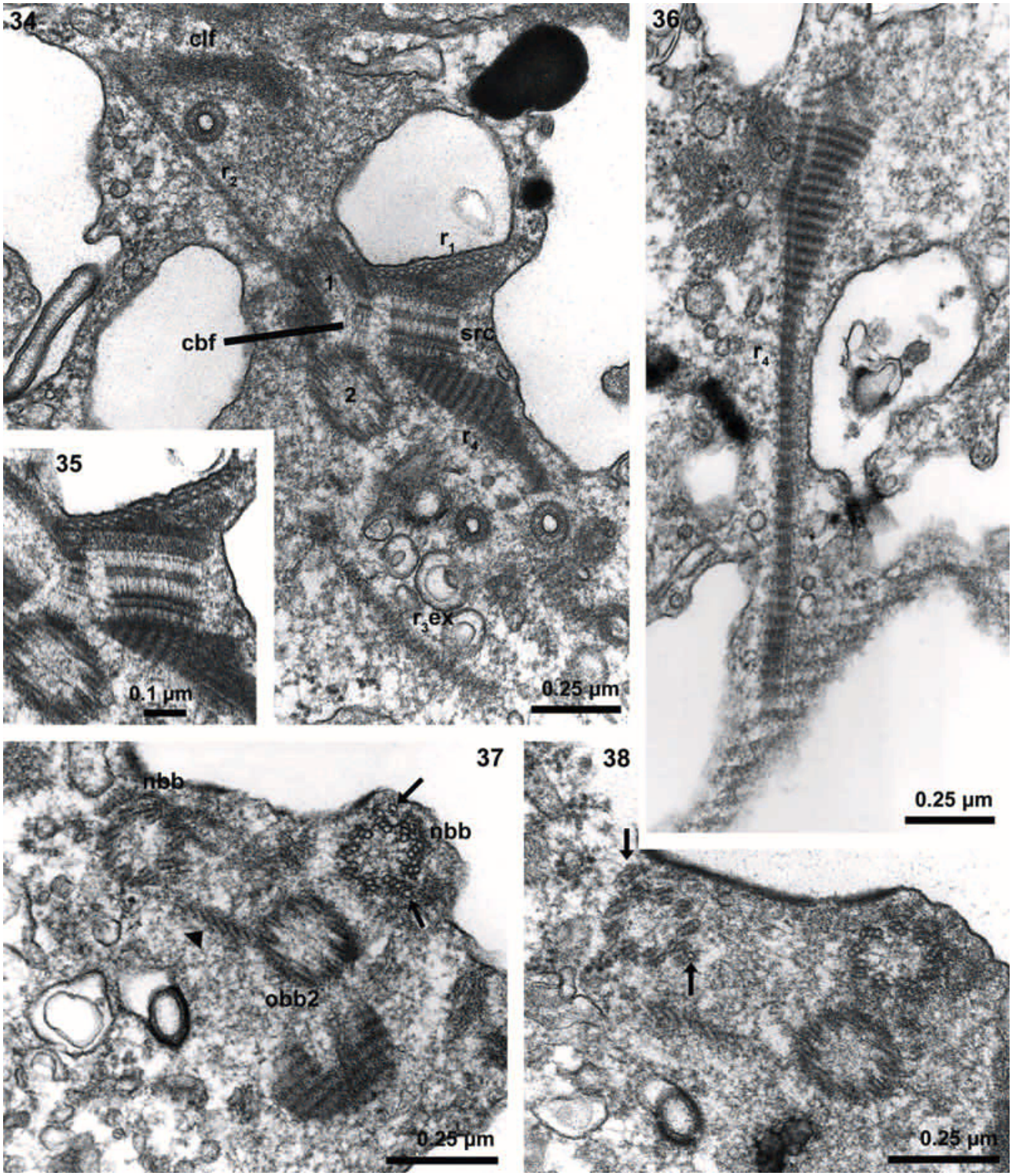


**Figs 34–38.** The flagellar apparatus and replication of basal bodies in *Biecheleriopsis adriatica* gen. et sp. nov. 34. Overview showing the two flagellar basal bodies (1 = lb, 2 = tb), the multitubular $r_1$ connected to the cross-banded $r_4$ by a conspicuous striated root connective (src), $r_2$ extending towards but apparently bypassing the collar of the longitudinal flagellum canal (clf), to terminate in the peripheral cytoskeleton of the cell, and finally the extension of $r_3$ ($r_3$ex). The cross-banded fiber (cbf) between the two basal bodies is also visible. 35. Higher magnification of the src area. 36. The cross-banded $r_4$ root from its emergence at the transverse flagellum basal body to its termination in the peripheral cytoskeleton of the cell. 37,38. Two sections from a cell in early flagellar replication. For further details, see the text. The arrows indicate single microtubules on the newly-formed basal bodies (centrioles), probably representing templates of new roots $r_3$ and $r_4$. The arrowhead marks a band of microtubules of unknown function located in the area between the original basal body of the transverse flagellum (obb2) and one of the new basal bodies (nbb).

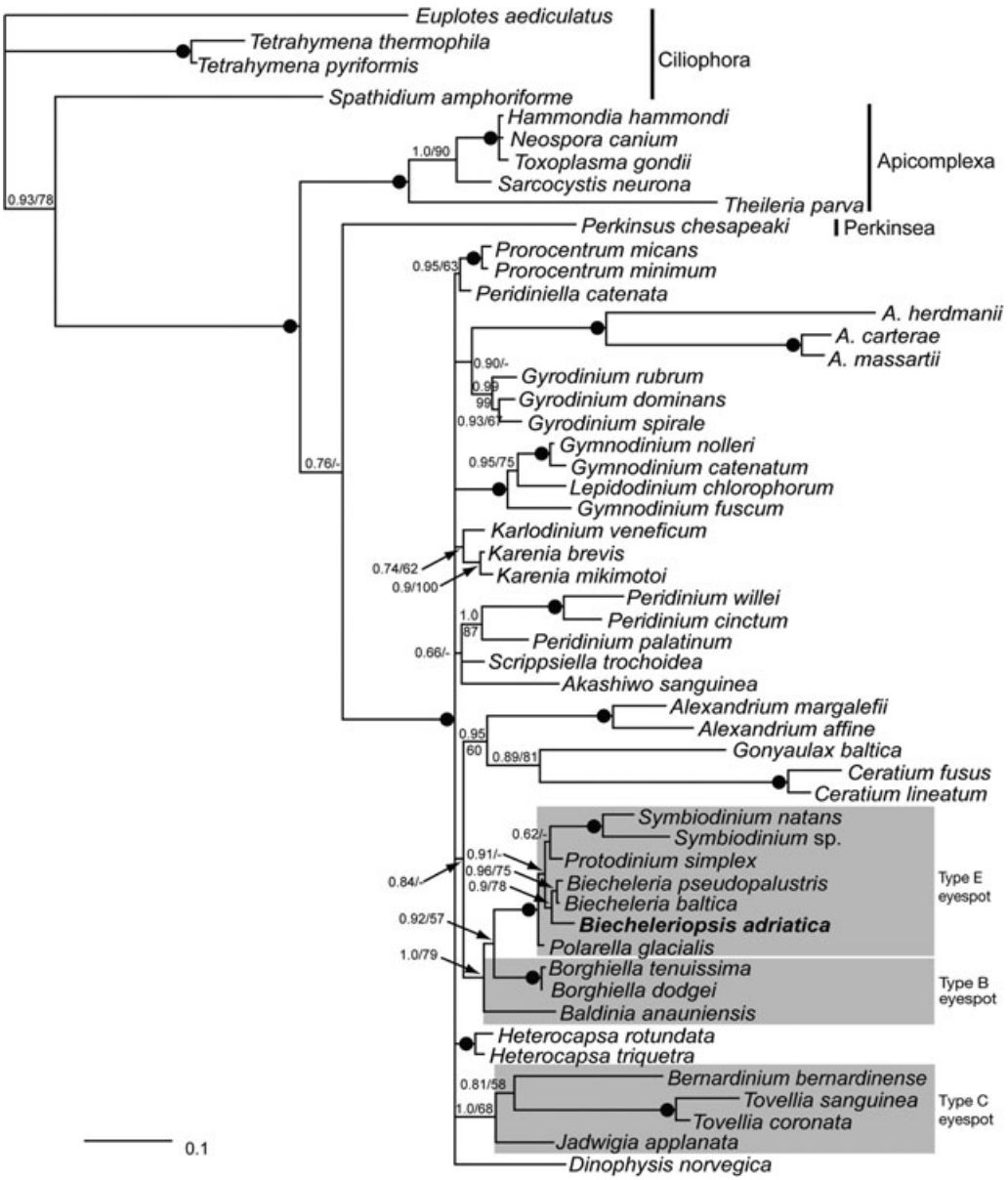


**Fig. 39.** Phylogeny of *Biecheleriopsis adriatica* gen. et sp. nov. based on partial, nuclear-encoded large subunit (LSU) rRNA sequences (1152 base pairs; excluding domain D2) and inferred from Bayesian analysis. The branch lengths are proportional to the number of substitutions per site. Four ciliates, five apicomplexa and the genus *Perkinsus* constituted the outgroup. Posterior probabilities (≤1) and bootstrap values (≥50%) from maximum likelihood bootstrap analyses (100 replications) using PhyML are written at internodes. A filled black circle is used to indicate the highest possible support value for the two phylogenetic methods applied. Three groups of woloszynskioid dinoflagellates, each defined by their specific type of eyespots (*sensu* Moestrup & Daugbjerg 2007) are indicated with grey boxes. *Biecheleriopsis adriatica* is marked in bold type to highlight its phylogenetic position. Due to space restrictions the three species assigned to the genus *Amphidinium* are abbreviated *A. herdmanii*, *A. carterae* and *A. massartii*.

single, low-magnification illustration. The text reads as follows:

'Minute and rotund species. Epicone shorter than hypocone. Girdle wide, impressed. Sulcus running straight up the epicone and over the apex so as to notch it slightly, widening posteriorly, overlapped on the left side by a tongue-like process. Flagella and pores not seen. Nucleus anterior. Several greenish chromatophores. Holophytic. Length 14 μm.

English Channel, half-way between Plymouth and the French coast. Several specimens in one sample. May, 1923'.

The IFREMER isolate agrees in size, relative sizes of the epi- and hypocone, and in having a distinct tongue-like process of the left ventral side of the hypocone. If differs in the nucleus being central and in the sulcus not extending to the apex. The sulcus extends for a short distance onto the epicone, and the continuation

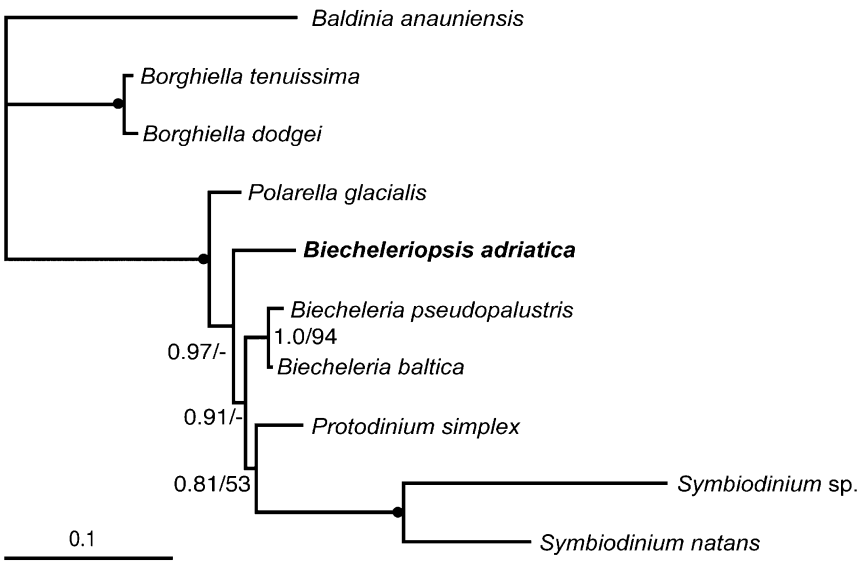


**Fig. 40.** Phylogeny of *Biecheleriopsis adriatica* gen. et sp. nov. based on partial, nuclear-encoded large subunit (LSU) rRNA sequences (1378 base pairs; including domain D2) and inferred from Bayesian analysis. The branch lengths are proportional to the number of substitutions per site. Based on the tree topology shown in Figure 39 *Baldinia anaueniensis* was chosen as the outgroup taxon. Posterior probabilities (≤1) and bootstrap values (≥50%) from maximum likelihood bootstrap analyses (100 replications) using PhyML are written at internodes. A filled black circle is used to indicate the highest possible support value for the two phylogenetic methods applied. *Biecheleriopsis adriatica* is marked in bold type to highlight its phylogenetic position.

seen by Lebour may have been the EAV. The IFREMER isolate is from the Adriatic Sea, while Lebour's material came from the Southern North Sea. Lebour described her material as greenish while our impression of the IFREMER material was a golden color. We do not consider this to be a real difference.

Dodge (1982) mentions that *Gymnodinium pygmaeum* may be an 'early report of what has come to be known as *Gyrodinium aureolum* Hulburt'. This is unlikely since *Gyrodinium aureolum* is much larger (24–40 μm long according to Dodge (1982)).

The IFREMER isolate is maintained at IFREMER as *Gymnodinium corii* Schiller. This species, which was described from spring plankton in the Adriatic, is somewhat similar but twice as large (27–30 μm rather than 12.5–15 μm) and without the distinct tongue-like process of the left ventral side of the hypocone. Cells of *Gymnodinium corii* were drawn by Schiller as covered by small plates (Schiller 1928, fig. 27a), indicating that this species may also be a woloszynskioid.

## The eyespot

The phylogenetic tree in Figure 39 indicates a phylogenetic relationship between *Biecheleriopsis* and a rather large, but well-defined assemblage of thin-walled dinoflagellates. This relationship is also borne out in the ultrastructure. The most characteristic feature of the assemblage is the structure of the eyespot, which has no known parallel in other dinoflagellates nor in any other protist. The eyespot is composed of a stack of cisternae resembling a Golgi body, and each cisterna contains brick-like structures. While the organelle is unlike a stigma in its ultrastructure, it resembles this organelle in its appearance in the light microscope and in its placement near the sulcus, associated with the descending microtubules of flagellar root $r_1$. It was termed Type E by Moestrup and Daugbjerg (2007) and it is, in addition to *Biecheleriopsis*, known from *Symbiodinium* (Hansen & Daugbjerg 2008), *Polarella* (Montresor *et al.* 1999), *B. baltica* (Kremp *et al.* 2005 as *Woloszynskia halophila*) and the tide-pool flagellate *Biecheleria natalensis* (Horiguchi & Pienaar 1994) (as *Gymnodinium natalense*). These species are related and should be placed in the same clade, the order Suessiales. A study of the function of the eyespot should be undertaken, and because of its rapid growth in culture *B. adriatica* would probably be suited for this purpose. An analogous type of photoreceptor has been found in the ciliate *Porpostoma notatum* (Kuhlmann *et al.* 1997). Rather than of separate cisternae it comprises numerous highly reflecting vacuoles, each containing a crystalline body. It has, however, a superficial resemblance to the eyespot of *Biecheleriopsis*.

## The amphiesma vesicles and the apical furrow apparatus

The anterior part of the dinoflagellate cell-covering is very diverse but there is little knowledge about the

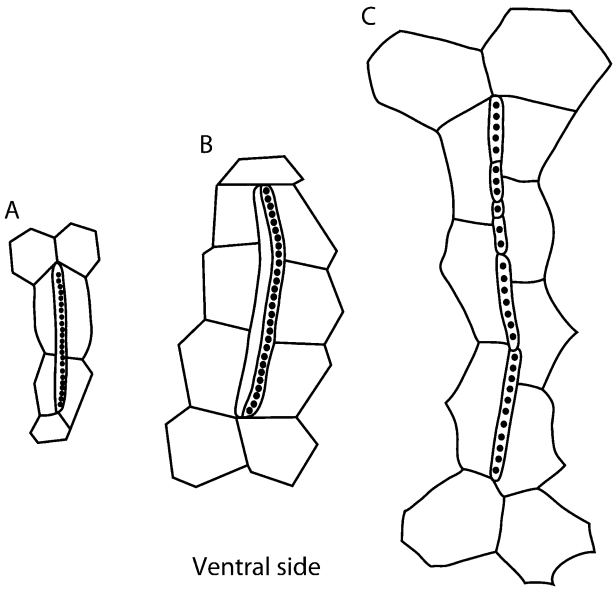


**Fig. 41.** Drawings of the apical furrow apparatus in woloszynskioids. (A) single elongate vesicle as in the Suessiaceae (*Biecheleria*, *Biecheleriopsis* and *Symbiodinium*, probably also *Protodinium*). (B) two elongate vesicles, one forming a furrow, as in the Borghiellaceae (*Borghiella*), (C) single line of vesicles as in the Tovelliaceae (*Tovellia* and *Jadwigia*).

functional significance of this diversity. Figure 41 illustrates in a diagrammatic form the three types of 'anterior furrow' or 'acrobase' we have found during our studies on woloszynskioids. The single EAV of *Biecheleriopsis adriatica* (Fig. 41A) is known also from motile cells of *Symbiodinium* (Loeblich III and Sherley 1979; Hansen & Daugbjerg 2008) and in *B. baltica* (Kremp *et al.* 2005) as *Woloszynskia halophila*; Moestrup *et al.* (2009). The elongate vesicle is typically 2–3 μm long and shows a central row of 12 (*Symbiodinium natans*: Hansen & Daugbjerg 2008) to 25 low projections (*B. baltica*, as *W. halophila*: Kremp *et al.* (2005)), most likely pore openings. In *B. pseudopalustre* the EAV is approximately 9 μm long and ornamented with more than 60 central knobs. It is not possible to determine the length of the EAV in *B. halophila*, as Biecheler (1952) (as *G. halophilum*) did not provide a scale.

Members of the Tovelliaceae, a somewhat remotely related family of dinoflagellates, are superficially similar but the apical apparatus in this family comprises a row of vesicles, each containing a distinct plate, in other words, an apical line of elongate plates (ALP *sensu* Lindberg *et al.* 2005) (Fig. 41C). The genus *Borghiella*, recently described by Moestrup *et al.* (2008), is also superficially similar but the apical apparatus comprises a pair of parallel elongate vesicles (Fig. 41B). One of the vesicles bears a central row of knobs and is undoubtedly the homolog of the single vesicle in the *Biecheleria–Symbiodinium* group, as documented by the identical internal support system of microtubules and opaque plates. It is difficult to evaluate the functional significance of the lack of an apical apparatus in the related forms *Polarella* and *Baldinia* (Montresor *et al.* 1999; Hansen *et al.* 2007). The thin-walled or naked dinoflagellates of *Gymnodinium*, *Gyrodinium*, *Akashiwo* and *Karlodinium* likewise possess an apical apparatus, which in *Karlodinium* comprises a deep (probably non-homologous) furrow, which is sufficiently wide to be visible in the light microscope (Daugbjerg *et al.* 2000). We refer to the light microscopy preparations of Biecheler (1952), using stained cells, to get an impression of the detailed structure of the apical furrow in *Gymnodinium*, since data based on SEM and TEM are lacking. Biecheler drew a single U-shaped amphiesmal vesicle with a central row of projections in the species identified as *Gyrodinium vorax* Biecheler (Biecheler 1952, 38, 40), most likely a species of *Gymnodinium*, and this may be the homolog of the single vesicle in *Biecheleria*.

## The nuclear connective

As mentioned above, the single most unusual feature of *Biecheleriopsis adriatica* is the nuclear connector, a fibrous structure that interconnects the flagellar apparatus and the nucleus. This structure, known from many groups of protists, for example, green algae and heterokonts (e.g. Moestrup 1982), occurs only sporadically in dinoflagellates. It was first discovered in *Polykrikos* by Bradbury *et al.* (1983), followed by reports in *Actiniscus* (Hansen 1993), *Nematodinium* (Roberts & Taylor 1995) and species of *Gymnodinium* (e.g. Roberts 1986; Hansen 2001). While *Gymnodinium* and *Polykrikos* are rather closely related (e.g. Hoppenrath & Leander 2007; Moestrup & Daugbjerg 2007), there is little information on the phylogenetic position of *Actiniscus* and *Nematodinium*. However, we have no indication that *Biecheleriopsis* is related to the *Gymnodinium–Polykrikos* group, which is also characterized by very peculiar chambers in the nuclear envelope, a feature not present in *Biecheleriopsis*. The nuclear connector – or rhizoplast as it was initially termed by Dangeard (1901) in *Polytomella* – maintains a close physical relation between the nucleus and the flagellar apparatus; the latter determining the position of many other organelles in the cell. A detailed study of mitosis in a dinoflagellate with a nuclear connector such as *Biecheleriopsis adriatica* would be of general interest.

## Why a new genus?

*Biecheleriopsis adriatica* is very similar to some species of *Biecheleria* and it may be argued that it should be included in that genus. Following extensive discussion, we have decided to erect a new genus for this species.

This conclusion is based on both morphological and molecular evidence. First, the presence of a nuclear connector is highly unusual and a similar structure has not been found in any species of *Biecheleria* studied so far. Second, close inspection of the second alignment of D2 revealed that *Biecheleria baltica* and *B. pseudopalustris* lacked a 51-base pair long fragment compared with the other dinoflagellates with type E and B eyespots (data not shown). This very significant deletion was missing approximately halfway down the second stem-loop of D2 *sensu* Lenaers *et al.* (1989) in their secondary structure model of the LSU rRNA of the thecate dinoflagellate *Prorocentrum micans*. The molecular synapomorphy highlights the close relationship between the two species of *Biecheleria* but at the same time separates them evolutionarily from *Biecheleriopsis adriatica*.

## Flagellar replication in dinoflagellates

Evidence is slowly accumulating on details of flagellar and flagellar root replication in dinoflagellates. In contrast to organelles such as nucleus, mitochondria and chloroplasts, which divide by division, the new flagellar bases arise *de novo* along the old flagella and flagellar bases. Some details are still missing but it is now well established that the two new basal bodies, at least in the dinoflagellate species examined so far, arise in parallel to or nearly so, and in the vicinity of, the transverse flagellum basal body. Both newly-formed basal bodies are associated with two single microtubules, located three (four) triplets apart. The position of the microtubules supports the contention that they represent root templates (immature roots), which during cytokinesis develop into the roots of the new transverse flagella (roots $r_3$ and $r_4$). The old transverse flagellum transforms into a longitudinal flagellum and the old roots $r_3$ and $r_4$ transform into roots $r_1$ and $r_2$. Flagellar replication in dinoflagellates was first reported in detail in *Prorocentrum* by Heimann *et al.* (1995), and chance sections obtained in other species (*Peridinium cinctum:* Calado *et al.* (1999) and *Borghiella*: Moestrup *et al.* (2008)) support the original observations. In *Biecheleriopsis*, the series from which Figures 37 and 38 have been taken shows two apparently identical new basal bodies – root complexes. The presence of a microtubular band located between the old transverse flagellum basal body and one of the new basal bodies still needs to be explained. The same configuration is visible in the micrograph of *Peridinium cinctum* published by Calado *et al.* (1999) and the microtubules are likely to play a role in the distribution of the new basal bodies to the daughter cells. Whether the band represents part of the old root system is unknown: perhaps the extension of the old root $r_3$?

## '*Gymnodinium* sp.' *sensu* Roberts (1986)

In one of his first articles on the flagellar apparatus in dinoflagellates, Roberts (1986) gave an account of *Gymnodinium* sp., a marine strain from University of Texas (UTEX) originally isolated by Loeblich. A comparison of the micrographs with those of *B. adriatica* leaves little doubt that '*Gymnodinium* sp.' is a close relative of *B. adriatica* and does not belong in *Gymnodinium*. It resembles *B. adriatica* in (i) the relative angle of the two basal bodies; (ii) the presence of a nuclear connector; (iii) the type of pusule; and (iv) flagellar details: most illustrations agree with *B. adriatica*, including small details such as the connective between the two basal bodies (sbc in Roberts 1986) and the banded structure that interconnects the ventral side of root $r_1$ with the collar of the longitudinal flagellum canal (v) the presence of brick-like material in cisternae in the cell (not commented upon by Roberts but visible in Figs 14–16). Cells of *Gymnodinium* sp. have the same size as *B. adriatica* but lack eyespot and pyrenoids, and *Gymnodinium* sp. has only four chloroplasts. The isolate was subsequently lost from UTEX and its identity remains uncertain until it can be found again. Most likely, it represents an undescribed species of *Biecheleriopsis*.

## ACKNOWLEDGMENTS

We thank Patrick Gentien and Evelyne Erard-Le Denn for supplying the strain of *Biecheleriopsis adriatica* from IFREMER, and Lisbeth Haukrogh for assisting with sectioning of the material for TEM. ND thanks Charlotte Hansen for help with the automated sequencing. We thank Stuart Sym for translating the diagnosis into Latin. This article is part of the project 'Biodiversity and phylogeny of dinoflagellates' supported financially by Villum Kann Rasmussen Foundation.

## REFERENCES

Biecheler, B. 1952. Recherches sur les Péridiniens. *Bull. Biol. de la France et de la Belgique* **36** (Suppl.):1–147.

Bradbury, P. C., Westfall, J. A. and Townsend, J. W. 1983. Ultrastructure of the dinoflagellate *Polykrikos*. 2. The nucleus and its connections to the flagellar apparatus. *J. Ultrstruct. Res.* **85**: 24–32.

Calado, A. J., Hansen, G. and Moestrup, Ø. 1999. Architecture of the flagellar apparatus and related structures in the type species of *Peridinium*, *P. cinctum* (Dinophyceae). *Eur. J. Phycol.* **34**: 179–91.

Dangeard, A. 1901. Étude comparative de la zoospore et du spermatozoïde. *C.R. Hebd. Seances Acad. Sci.* **132**: 859–61.

Daugbjerg, N., Moestrup, Ø. and Arctander, P. 1994. Phylogeny of the genus *Pyramimonas* (Prasinophyceae) inferred from the *rbc*L gene. *J. Phycol.* **30**: 991–9.

Daugbjerg, N., Hansen, G., Larsen, J. and Moestrup, Ø. 2000. Phylogeny of some of the major genera of dinoflagellates based on ultrastructure and partial LSU rDNA sequence data, including the erection of three new genera of unarmoured dinoflagellates. *Phycologia* **39**: 302–17.

Dodge, J. D. 1982. *Marine Dinoflagellates of the British Isles*. Her Majesty's Stationery Office, London, 303 pp.

Felsenstein, J. 2008. *PHYLIP (Phylogeny Inference Package)*, version 3.68. Distributed by the author. Department of Genome Sciences, University of Washington, Seattle, WA.

Guindon, S. and Gascuel, O. 2003. A simple, fast, and accurate algorithm to estimate large phylogenies by maximum likelihood. *Syst. Biol.* **52**: 696–704.

Hansen, G. 1993. Light- and electron microscopical observations on the dinoflagellate *Actiniscus pentasterias* (Dinophyceae). *J. Phycol.* **29**: 486–99.

Hansen, G. 2001. Ultrastructure of *Gymnodinium aureolum* (Dinophyceae). Toward a further redefinition of *Gymnodinium sensu stricto*. *J. Phycol.* **37**: 612–23.

Hansen, G. and Daugbjerg, N. 2008. *Symbiodinium natans* sp. nov. – a free-living dinoflagellate from Tenerife (mid Atlantic Ocean). *J. Phycol.* **45**: 251–63.

Hansen, G., Daugbjerg, N. and Henriksen, P. 2007. *Baldinia anauniensis* gen. et sp. nov.: a 'new' dinoflagellate from Lake Tovel, N. Italy. *Phycologia* **46**: 86–108.

Heimann, K., Roberts, K. R. and Wetherbee, R. 1995. Flagellar apparatus transformation and development in *Prorocentrum micans* and *P. minimum* (Dinophyceae). *Phycologia* **34**: 323–35.

Hoppenrath, M. and Leander, B. S. 2007. Morphology and phylogeny of the pseudocolonial dinoflagellates *Polykrikos lebourae* and *Polykrikos herdmanae* n. sp. *Protist* **158**: 209–27.

Horiguchi, T. and Pienaar, R. N. 1994. *Gymnodinium natalense* sp. nov. (Dinophyceae), a new tide pool dinoflagellate from South Africa. *Jpn J. Phycol.* **42**: 21–8.

Kremp, A., Elbrächter, M., Schweikert, M., Wolny, J. L. and Gottschling, M. 2005. *Woloszynskia halophila* (Biecheler) comb. nov.: a bloom-forming cold-water dinoflagellate co-occurring with *Scrippsiella hangoei* (Dinophyceae) in the Baltic Sea. *J. Phycol.* **41**: 629–42.

Kuhlmann, H.-W., Bräucker, R. and Schepers, A. G. 1997. Phototaxis in *Porpostoma notatum*, a marine scuticociliate with a composed crystalline organelle. *Eur. J. Protistol.* **33**: 295–304.

Lebour, M. V. 1925. *The Dinoflagellates of the Northern Seas*. Marine Biological Association of the United Kingdom, Plymouth, pp. 1–250.

Lenaers, G., Maroteaux, L., Michot, B. and Herzog, M. 1989. Dinoflagellates in evolution. A molecular phylogenetic analysis of large subunit ribosomal RNA. *J. Mol. Ecol.* **29**: 40–51.

Lindberg, K., Moestrup, Ø. and Daugbjerg, N. 2005. Studies on woloszynskioid dinoflagellates I: *Woloszynskia coronata* re-examined using light and electron microscopy and partial LSU rDNA sequences, with description of *Tovellia* gen. nov. and *Jadwigia* gen. nov. (Tovelliaceae fam. nov.). *Phycologia* **44**: 416–40.

Loeblich, A. R. III and Sherley, J. L. 1979. Observations on the theca of the motile phase of free-living and symbiotic isolates of *Zooxanthella microadriatica* (Freudenthal) comb. nov. *J. Mar. Biol. Assoc. UK* **59**: 195–205.

Moestrup, Ø. 1982. Phycological reviews. 7. Flagellar structure in algae – a review with new observations particularly on the Chrysophyceae, Phaeophyceae (Fucophyceae), Euglenophyceae, and *Reckertia*. *Phycologia* **21**: 427–528.

Moestrup, Ø. 2000. The flagellate cytoskeleton. *In* Leadbeater, B. S. C. and Green, J. C. (Eds) *The Flagellates, Unity, Diversity and Evolution*. Taylor and Francis, London, pp. 69–94.

Moestrup, Ø. and Daugbjerg, N. 2007. On dinoflagellate phylogeny and classification. *In* Brodie, J. and Lewis, J. (Eds) *Unravelling the Algae, the Past, Present and Future of Algal Systematics*. CRC Press, Taylor and Francis Group, Boca Raton, FL, pp. 215–30.

Moestrup, Ø., Hansen, G. and Daugbjerg, N. 2008. Studies on woloszynskioid dinoflagellates III: on the ultrastructure and phylogeny of *Borghiella dodgei* gen. et sp. nov., a cold-water species from Lake Tovel, N. Italy, and on *B. tenuissima* comb. nov. (syn. *Woloszynskia tenuissima*). *Phycologia* **47**: 54–78.

Moestrup, Ø., Lindberg, K. and Daugbjerg, N. 2009. Studies on woloszynskioid dinoflagellates IV: the genus *Biecheleria* gen. nov. *Phycol. Res.* **57**: 203–220 (in press).

Montresor, M., Procaccini, G. and Stoecker, D. 1999. *Polarella glacialis*, gen. nov., sp. nov. (Dinophyceae): Suessiaceae are still alive! *J. Phycol.* **35**: 186–97.

Nylander, J. A. A. 2004. *MrModeltest*, v2. Program distributed by the author. Evolutionary Biology Centre, Uppsala University.

Roberts, K. R. 1986. The flagellar apparatus of *Gymnodinium* sp. *J. Phycol.* **22**: 456–66.

Roberts, K. R. and Taylor, F. J. R. 1995. The flagellar apparatus of *Nematodinium armatum*. *J. Phycol.* **34** (Suppl.): 51.

Ronquist, F. and Huelsenbeck, J. P. 2003. MRBAYES 3: Bayesian phylogenetic inference under mixed models. *Bioinformatics* **19**: 1572–4.

Schiller, J. 1928. Die planktischen Vegetationen des adriatischen Meeres. C. Dinoflagellata. 2. Theil. Gymnodiniales. *Arch. Protistenk.* **61**: 119–66.

Scholin, C. A., Herzog, M., Sogin, M. and Anderson, D. M. 1994. Identification of group- and strain-specific genetic markers for globally distributed *Alexandrium* (Dinophyceae). II. Sequence analysis of a fragment of the LSU rRNA gene. *J. Phycol.* **30**: 999–1011.

Swofford, D. L. 2003. *PAUP* Phylogenetic Analysis Using Parsimony (*and Other Methods)*, version 4. Sinauer Associates, Sunderland, MA.

Wilgenbusch, J. C., Warren, D. L. and Swofford, D. L. 2004. *AWTY: A system for graphical exploration of MCMC convergence in Bayesian phylogenetic inference*. Available at: http://ceb.csit.fsu.edu/awty